

## Optical Torque Wrench: Angular Trapping, Rotation, and Torque Detection of Quartz Microparticles

Arthur La Porta and Michelle D. Wang

*Department of Physics, Laboratory of Atomic and Solid State Physics, Cornell University, Ithaca, New York 14853, USA*

(Received 14 August 2003; published 14 May 2004)

We describe an apparatus that can measure the instantaneous angular displacement and torque applied to a quartz particle which is angularly trapped. Torque is measured by detecting the change in angular momentum of the transmitted trap beam. The rotational Brownian motion of the trapped particle and its power spectral density are used to determine the angular trap stiffness. The apparatus features a feedback control that clamps torque or other rotational quantities. The torque sensitivity demonstrated is ideal for the study of known biological molecular motors.

DOI: 10.1103/PhysRevLett.92.190801

PACS numbers: 07.60.-j, 05.40.Jc, 42.79.-e, 87.80.Cc

Optical tweezers have made critical contributions to the creation of a vibrant field of biophysical research—single molecule manipulation of nucleic acids and protein complexes [1,2]. Although the possibility of manipulating biological objects was readily appreciated [3], the true potential of optical tweezers was realized only when microspheres were used as handles to displace attached biomolecules and measure the resulting force [4,5]. It would be equally useful to have a handle that could be used to *rotate* biological structures and to precisely measure the associated *torque*. Here we demonstrate angular trapping and torque detection using nominally spherical but anisotropic quartz particles. The torque acting on the particle and its deviation from the trap direction are determined by direct measurement of the change in angular momentum of the transmitted beam. The ability to measure instantaneous torque is of great importance, since it will facilitate precise measurement of the torque generated by biological structures as they rotate. The wide bandwidth and accuracy of our detection scheme allow us to measure Brownian rotational motion of the trapped particle and to use feedback to control the applied torque or particle angle.

Several other techniques have been demonstrated for rotating microscopic particles. These include use of azimuthally asymmetric beams or combinations of beams to rotate nonspherical particles [6–8], use of linearly or circularly polarized light to orient or apply torque to birefringent calcite particles [9], or use of magnetic fields to apply torque to free or optically trapped magnetic particles [10,11]. The technique we demonstrate here is similar to that employed by Friese *et al.*, but with the important advantage that angular trapping is combined with a detector allowing instantaneous measurement of the torque acting on the particle and its angular deviation from the trap direction. Using an optical power of  $\sim 10$  mW, the trap is capable of rotating micron size particles with angular velocities up to 200 rad/s and generating several hundred pN · nm of torque. The reso-

lutions of torque measurement and angular confinement are limited by rotational Brownian motion of the particle.

The angular trap is based on the fact that a dielectric material subject to an external electric field  $\mathbf{E}$  (constant or oscillating) generates polarization  $\mathbf{P}$  given by  $\mathbf{P} = \chi\mathbf{E}$ , where  $\chi$  is the electric susceptibility. If the material is birefringent, the susceptibility is not isotropic so that the expression for the polarization is generalized to  $\mathbf{P} = \chi_x E_x \hat{x} + \chi_y E_y \hat{y} + \chi_z E_z \hat{z}$ , where  $\hat{x}$ ,  $\hat{y}$ , and  $\hat{z}$  are unit vectors along the principal axes of the crystal and  $\chi_x$ ,  $\chi_y$ , and  $\chi_z$  are the corresponding electrical susceptibilities [12]. For typical uniaxial birefringent materials such as quartz or calcite, two of the susceptibilities are equal ( $\chi_o$  ordinary) and the third is different ( $\chi_e$  extraordinary).

Angular trapping occurs in particles made from materials such as quartz, in which the extraordinary axis of the crystal is more easily polarized than the ordinary axes. In this case the polarization  $\mathbf{P}$  induced on a particle by an external electric field  $\mathbf{E}$  will be tilted toward the extraordinary axis, as illustrated in Fig. 1(a). The misalignment between  $\mathbf{E}$  and  $\mathbf{P}$  results in a torque given by

$$\begin{aligned} \boldsymbol{\tau} &= \int d^3x \mathbf{P} \times \mathbf{E} \\ &= \hat{q} \frac{1}{2} (\chi_o - \chi_e) \sin 2\theta \int d^3x E_0^2(\mathbf{x}) = \hat{q} \tau_0 \sin 2\theta, \end{aligned} \quad (1)$$

where  $\theta$  is the angle between  $\mathbf{E}$  and the extraordinary axis,  $\hat{q}$  is a unit vector perpendicular to  $\mathbf{E}$  and  $\mathbf{P}$ , and  $\tau_0$  is the maximum magnitude of torque that can be exerted on the particle. (Particle shape effects are neglected in this formula.) As a result, linearly polarized light can be used to exert torque on a quartz particle. This torque tends to align the extraordinary axis of the quartz particle with the electric field direction, as shown by the quartz sphere in Fig. 1(b). Materials such as calcite, where the extraordinary axis is less polarizable than the ordinary axes, will experience torque [9] but have additional rotational degrees of freedom, as illustrated by the calcite spheres in Fig. 1(b).

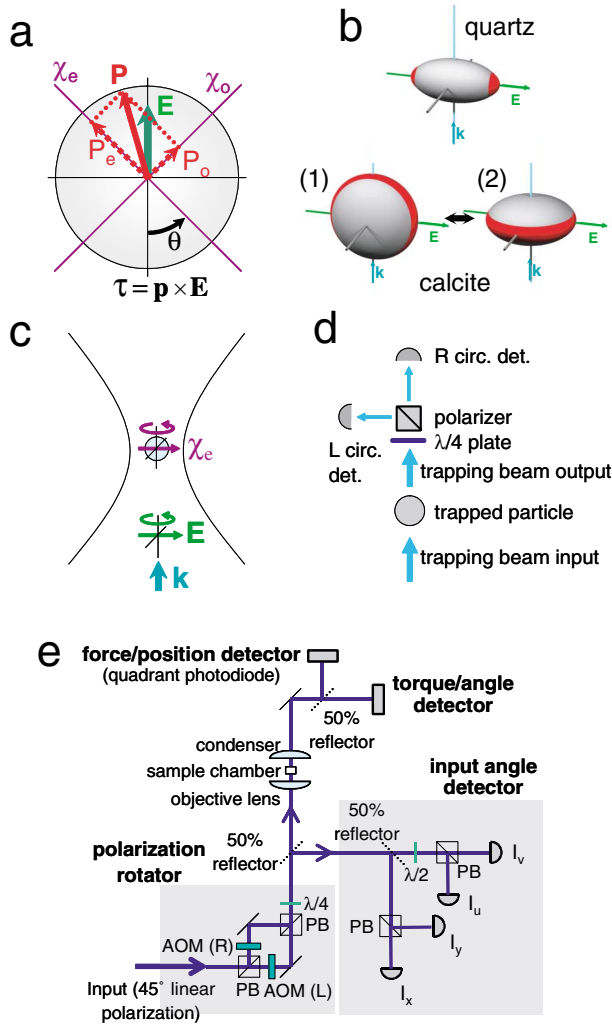


FIG. 1 (color). (a) Polarization vector  $\mathbf{P}$  induced in an anisotropic particle by an external electric field  $\mathbf{E}$ . Torque is generated when  $\mathbf{P}$  is not aligned with the field. (b) The index ellipsoids of quartz and calcite are represented, where the region of maximum electric susceptibility is marked in red. Torque exerted on the particle tends to align the red region with the  $\mathbf{E}$  vector. For quartz particles the applied torque tends to align the extraordinary axis (red areas) with the  $\mathbf{E}$  vector, constraining two of three Euler angles. For calcite particles, the extraordinary axis is repelled by the  $\mathbf{E}$  vector and the plane defined by the ordinary axes (red band) is attracted to the  $\mathbf{E}$  field, constraining one of three Euler angles. In this case the extraordinary axis is either perpendicular [ellipsoid marked (1)] or parallel to the propagation vector  $\mathbf{k}$  [ellipsoid marked (2)]. In the latter case, the birefringence of the particle is extinguished, allowing the particle to spin freely around the optical axis (along  $\mathbf{k}$ ). (c) The alignment of the particle with the trap polarization is illustrated. (d) The torque detector measures the difference in intensities of the right circular and left circular components of the transmitted beam. (e) Schematic representation of the apparatus. The polarization rotator is described in the text. The input detector determines the polarization angle of the input trapping field. The torque detector and quadrant detector determine the torque and force acting on the particle.

In order to detect the torque we take advantage of the conservation of angular momentum, which requires that the torque acting on the particle is equal and opposite to the rate of change of the angular momentum of the trapping beam as it passes through the particle. Since the torque is generated using polarization properties rather than the shape of the beam or particle, the angular momentum is transferred to the polarization state of the transmitted beam rather than to its spatial profile. Light with left-handed (right-handed) circular polarization contains angular momentum  $+\hbar$  ( $-\hbar$ ) and energy  $\hbar\omega_0$  per photon, where  $\hbar$  is the reduced Planck constant and  $\omega_0$  is the optical angular frequency. The linearly polarized input trap beam contains no net angular momentum because it is composed of equal quantities of left and right circular polarization. Exertion of torque  $\tau$  on a particle causes an imbalance of the power of left and right circular components ( $P_L$  and  $P_R$ ) in the transmitted beam, such that  $\tau = (P_R - P_L)/\omega_0$ . Direct measurement of this quantity is made by the torque detector shown in Fig. 1(d). In principle, the torque is strictly determined by the angular momentum content of the transmitted beam [13]. In practice, it is impossible to collect the transmitted trap beam in its entirety, so a calibration of the detector is necessary.

To manipulate the particle angle it is necessary to have precise and rapid control of the trap polarization angle. Such control is impractical using mechanical means and is instead accomplished by the polarization rotator shown in Fig. 1(e). In this device the acousto-optic modulators (AOMs) marked L and R generate the left and right circular components of the output beam, and the relative phase of these components is determined by the relative phase shift  $\phi$  of the rf signals causes a rotation of  $\phi/2$  of the output polarization. The AOM drive signals are generated by computer-controlled digital frequency synthesis, allowing the polarization angle to be changed with a response time of a few microseconds. Also shown in Fig. 1(e) are the detectors used to measure the input polarization angle, the torque, and the linear displacement of the trapped particle.

The rotation of a small quartz particle using the apparatus is shown in Fig. 2. The particle shown has a

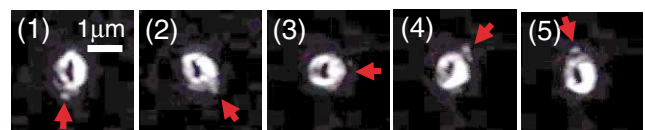


FIG. 2 (color). Video images recorded every 250 ms show a  $\sim 1 \mu\text{m}$  diameter quartz particle being rotated counterclockwise in the angular trap. Quartz particles are obtained by centrifuging and collecting fractions from quartz powder. The particle shown is close to spherical but has an irregularity on one side (indicated by arrows) that allows its orientation to be recognized in video images.

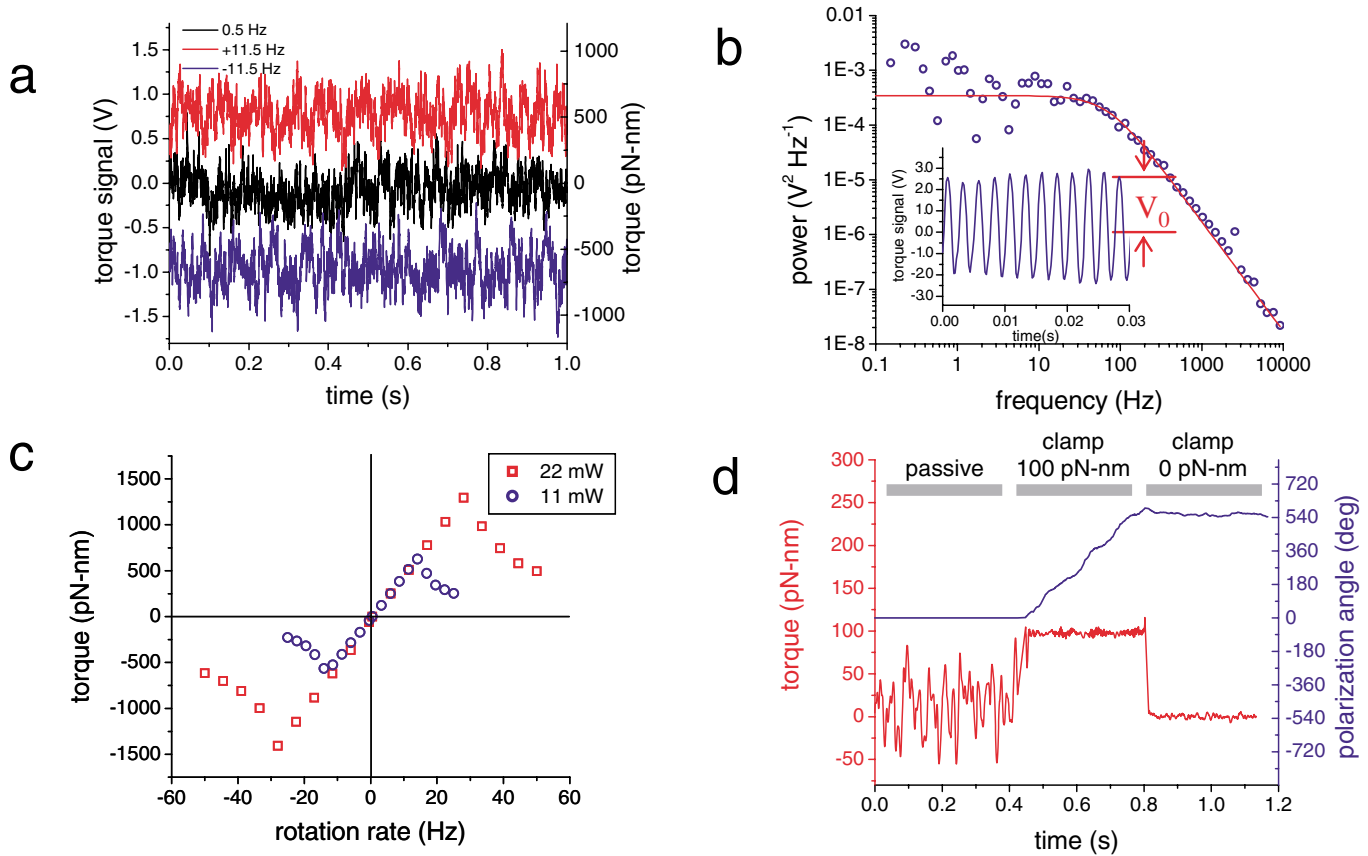


FIG. 3 (color). (a) The torque signal for a particle spinning in opposite directions at 11.5 rps, and nearly motionless at 0.5 rps. The dc offset is a measure of the drag on the spinning particle and the broadband fluctuations are primarily due to Brownian motion. (b) The power spectral density of the rotational fluctuations, and fit with Lorentzian function of the form  $S(f) = A^2/(f^2 + f_0^2)$  with  $A^2 = 0.059 \text{ rad}^2 (\text{Hz})$  and  $f_0 = 75 \text{ Hz}$ . The inset shows the torque signal as a quasistationary particle is scanned by a rapidly rotating polarization vector (200 Hz). The amplitude  $V_0 = 2.63 \text{ V}$  implies a small-signal angle sensitivity of  $0.19 \text{ rad/V}$ . From these values we calculate stiffness  $\kappa = 3360 \text{ pN} \cdot \text{nm}/\text{rad}$ , damping coefficient  $\xi = 7.1 \text{ pN} \cdot \text{nm} \cdot \text{s}$ , and torque sensitivity  $638 \text{ pN} \cdot \text{nm}/\text{V}$ . (c) The measured torque as a function of rotation rate, converted to  $\text{pN} \cdot \text{nm}$  using the calibration parameters defined in (b). From the slope of the linear regime we obtain  $\xi = 7.8 \text{ pN} \cdot \text{nm} \cdot \text{s}$ . (d) Measured torque and trap polarization angle as a function of time. Feedback to stabilize the torque at  $100 \text{ pN} \cdot \text{nm}$  ( $0 \text{ pN} \cdot \text{nm}$ ) is activated at  $0.4 \text{ s}$  ( $0.8 \text{ s}$ ).

noticeable deviation from spherical shape, allowing the rotation of the particle to be confirmed visually. Particles which are spherical in shape can also be rotated, as can be determined using the torque detector, which also measures angular displacement.

The measurement of the torque acting on a particle spinning at uniform velocity is shown in Fig. 3(a). The three traces show broadband fluctuations with different mean values. The fluctuations arise from Brownian rotational motion of the particle, as discussed below. The mean value, which is zero in the absence of rotation and is positive or negative for counterclockwise or clockwise rotation, is a measure of the viscous drag on the spinning particle.

The first step in the calibration procedure is to relate the torque signal to the deviation of the particle from the trap polarization angle. Referring to Eq. (1) we find that the angle is given by  $\theta = (1/2) \arcsin(V_\tau/V_0)$ , where  $V_\tau$  is the torque signal in volts and  $V_0$  is the maximum value of

this signal, obtained at  $\theta = 45^\circ$ . The value of  $V_0$  may be determined by rotating the polarization much faster than the particle can follow, so that the polarization vector scans the quasistationary particle. The amplitude of the resulting sinusoidal modulation is  $V_0$  [see Fig. 3(b) inset]. For small angles we can approximate  $\theta \approx V_\tau/2V_0$ .

Once the angular calibration is accomplished, angular deviation can be determined from the torque signal. The task remains to determine the stiffness of the angular trap and convert the torque signal to physical units of torque. Applying the standard treatment of Brownian fluctuations in a potential well to rotational motion [14], we find that the power spectral density of the angular fluctuations is of the form  $S(f) = A^2/(f^2 + f_0^2)$  with corner frequency  $f_0 = \kappa/2\pi\xi$  and amplitude  $A^2 = k_B T/\xi\pi^2$ , where  $k_B$  is the Boltzmann constant,  $T$  is the temperature in degrees kelvin,  $\kappa$  is the stiffness of the angular trap, and  $\xi$  is the rotational viscous damping coefficient. The damping  $\xi$  and stiffness  $\kappa$  are determined

by fitting the predicted function to the measured power spectrum, shown in Fig. 3(b). Once the angular trap stiffness is known the torque is related to the raw torque by  $\tau = V_\tau(\kappa/2V_0)$ . The torque sensitivity obtained from the calibration is within experimental error of the absolute angular momentum change of the trap beam, taking into account our estimated  $\sim 50\%$  light collection efficiency.

The calibration of torque allows us to directly measure the viscous drag on a spinning particle as a function of rotation rate. Figure 3(c) shows this function measured using two different values of the trap power. As expected, the two traces show a regime of linear scaling of torque with rotation rate having identical slope. The drag coefficient obtained from this slope is within experimental uncertainty of the value obtained from Brownian motion (see the Fig. 3 caption). For a spherical particle in an infinite fluid volume, we expect  $\xi = \pi\eta D^3$ , where  $D$  is the particle diameter and  $\eta$  is the viscosity of water. Using the measured  $\xi$  we obtain  $D = 1.3 \mu\text{m}$ , which is consistent with the apparent particle size in Fig. 2. For both power levels the linear scaling fails above the rotation rate where the torque needed to spin the particle exceeds the maximum torque available.

Finally, in Fig. 3(d) we demonstrate active stabilization of the torque using feedback to the polarization angle. During the initial part of the trace the trap polarization was held constant and Brownian fluctuations of the torque were observed. At 0.4 s a computer-controlled servo loop was activated which adjusted the polarization angle to maintain a constant torque of 100 pN · nm on the particle, and at 0.8 s the setpoint was reduced to 0 pN · nm. During active feedback the polarization angle is varied rapidly to suppress torque fluctuations. Although we have demonstrated this feedback technique using free particles, it can also be used to stabilize torque (or another variable such as particle orientation) against an active load such as a molecular motor.

We anticipate that the system we have developed will be well suited for measurements of torque and rotation in single molecule biological systems. Quartz surfaces may be functionalized for biomolecule attachment using standard techniques [15], and material processing techniques may be employed to make the particles more regular in shape [16]. Molecular motors are known to generate torque ranging from tens to thousands of pN · nm

[17,18], which is well within the dynamic range of the apparatus without requiring excessive trap power. Most importantly, the instantaneous readout and feedback capabilities will allow the torque generated by a biological structure in response to the imposed rotation (or vice versa) to be continuously measured.

We thank Professor R. H. Silsbee for stimulating scientific discussions. This work was supported by grants from NIH, the Keck Foundation, and by the STC program of the NFS under Agreement No. ECS-9876771.

- 
- [1] C. Bustamante, J. J. Macosko, and G. J. Wuite, *Nat. Rev. Mol. Cell. Biol.* **1**, 130 (2000).
  - [2] M. D. Wang, *Curr. Opin. Biotechnol.* **10**, 81 (1999).
  - [3] A. Ashkin and J. M. Dziedzic, *Science* **235**, 1517 (1987).
  - [4] K. Svoboda, C. F. Schmidt, B. J. Schnapp, and S. M. Block, *Nature (London)* **365**, 721 (1993).
  - [5] M. D. Wang *et al.*, *Science* **282**, 902 (1998).
  - [6] A. T. O'Neil and M. J. Padgett, *Opt. Lett.* **27**, 743 (2002).
  - [7] L. Paterson, M. P. MacDonald, J. Arlt, W. Sibbet, P. E. Bryant, and K. Dholakia, *Science* **292**, 912 (2001).
  - [8] V. Bingelyte, J. Leach, J. Courtial, and M. J. Padgett, *Appl. Phys. Lett.* **82**, 829 (2003).
  - [9] M. E. J. Friese, T. A. Nieminen, N. R. Heckenberg, and H. Rubinsztein-Dunlop, *Nature (London)* **394**, 348 (1998).
  - [10] L. Sacconi *et al.*, *Opt. Lett.* **26**, 1359 (2001).
  - [11] T. R. Strick, V. Croquette, and D. Bensimon, *Nature (London)* **404**, 901 (2000).
  - [12] A. Yariv, *Optical Electronics* (Holt, Rinehart, and Winston, New York, 1985).
  - [13] T. A. Nieminen, N. R. Heckenberg, and H. Rubinsztein-Dunlop, *J. Mod. Opt.* **48**, 405 (2001). After the submission of our manuscript a similar detector configuration was published in A. I. Bishop, T. A. Nieminen, N. R. Heckenberg, and H. Rubinsztein-Dunlop, *Phys. Rev. A* **68**, 033802 (2003).
  - [14] K. Svoboda and S. M. Block, *Annu. Rev. Biophys. Biomol. Struct.* **23**, 247 (1994).
  - [15] D. Kleinfeld, K. H. Kahler, and P. E. Hockberger, *J. Neurosci.* **8**, 4098 (1988).
  - [16] H. T. Sun, Z. T. Cheng, X. Yao, and W. Wlodarski, *Sens. Actuators B* **13**, 107 (1993).
  - [17] H. Noji, R. Yasuda, M. Yoshida, and K. Kinoshita, *Nature (London)* **386**, 299 (1997).
  - [18] W. S. Ryu, R. M. Berry, and H. C. Berg, *Nature (London)* **403**, 444 (2000).